Jurnal Teknologi

Full Paper

FREQUENCY OF NON-LINEAR DYNAMIC RESPONSE OF A POROUS FUNCTIONALLY GRADED CYLINDRICAL PANELS

Ahmed Mouthanna[a]*, Sadeq H. Bakhy[a], Muhannad Al-Waily[b]

[a]University of Technology, Mechanical Engineering Department, Iraq
[b]Department of Mechanical Engineering, Faculty of Engineering, University of Kufa, Iraq

Article history
Received
14 March 2022
Received in revised form
26 July 2022
Accepted
28 Juy 2022
Published Online
23 October 2022

*Corresponding author
me.20.26@grad.uotechnology.edu.iq

Graphical abstract

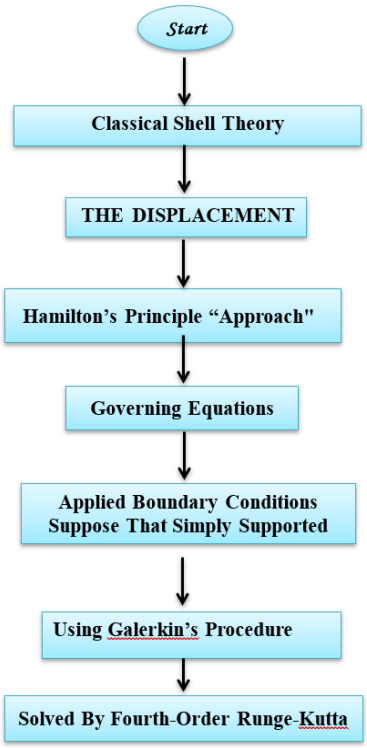

Abstract

In this article, a nonlinear dynamical investigation of porose functionally graded cylindrical panels using a proposed analytical model is carried out. The material's properties are considered to be porosity-dependent and graded in the thickness direction, corresponding to a power-law distribution. The classical shell theory, with the geometrical shape of nonlinear in von Karman–Donnell, is employed to get the Lagrange motion equations. By applying the Galerkin procedure, the system of nonlinear dynamic vibration equations is found. The natural frequencies and dynamic amplitude vibrations are obtained by using the fourth-order Runge–Kutta approach. In numerical analyses, the effects of porosity factor, power-law index, porous FGM thickness, frequency–amplitude relation, and excitation force on the dynamic response of thin functionally graded porous cylindrical panels are investigated. Through the obtained results, it is discovered that the porosity coefficients have important effects on the natural frequencies and amplitude of the nonlinear dynamic response of the FG structures. It leads to a reduction in natural frequencies by 5.74 % at 10% pores.

Keywords: Non-linear vibration, Galerkin technique, porous functionally graded Materials, shell theory, cylindrical Panels

1.0 INTRODUCTION

The cylindrical shell structures are numerously used as structural common components in different engineering areas involving aircraft engineering, aerospace engineering, and nuclear reactors [1]. In general, "functionally graded materials (FGMs)" can be divided into three categories: microstructural

gradients, chemical composition gradients, and porosity gradients [2]. The porous functionally graded material (PFGM) is one of the promising materials for these applications because it has excellent properties compared to other compounds, such as energy absorption potential, high strength, and low thermal conductivity [3]. Previous investigations studied the behavior of the mechanical properties of laminated composites and isotropic cylindrical shells [4]–[7]. Free vibration of a cylindrical shell is of significant interest for manufacturing and engineering design and has been considerably investigated by extant studies [8]–[11]. Loy *et al*. [12] investigated the vibration behavior of the cylindrical shells made of FGM, consisting of nickel and stainless steel. Bach [13] has an analytical study and used some well-known principles of nonlinear shallow shells to derive the governing equations. Chorfi and Houmat [14] adopted the first-order shear deformation theory (FSDT) with Von Karman's assumptions, to study the non-linear free vibration of the FGM thick elliptical plan-form shallow shell by utilizing the (p-version) finite element method (FEM) and the blending function method. Mouthanna *et al.* [15] provided an analytical examination of the non-linear natural frequencies of FG cylindrical panels subjected to the influence of various stiffeners' geometric shapes. Shi-Rong Li *et al*. [16] studied the free vibration of the circular shell with simply supported boundary conditions, the core formed of FGM, and the two outer surfaces made from the same homogeneous material. Bich *et al*. [17] presented an analytical approach to examine critical dynamic loads or stability and nonlinear dynamical responses of smeared eccentrically stiffened functionally graded material (ES-FGM) of cylindrical panels. Duc and Quan [18] investigated the nonlinear response of eccentrically stiffened cylindrical panels affected by mechanical loads resting on elastic foundations. Di Wu *et al*. [19] offered a numerical method to study the free and forced vibration of FG porous beams by using the finite element method. Akbaş [20] employed the Hamilton method and the finite element method to analyze forced vibration responses for FG porous beams subjected to dynamic load with porosity influences. Haichao Li [21] offered a semi-analytical solution by adopting Jacobi polynomials and Fourier series to investigate the characteristics of free vibration of the FG porous cylindrical shell under various boundary conditions. Barati and Zenkour [22] presented an analytical approach to investigate the characteristics of free vibrational for cylindrical shells formed of FG porous reinforced with graphene platelets resting on Winkler and Pasternak foundations. Akbaş *et al*. [23] conducted a numerical approach to analyze the vibration response of porous functionally graded thick beams subject to sine pulse load, including the damping influence, by applying a finite element model. Shahgholian *et al*. [24] adopted first order shear deformation theory and the Rayleigh-Ritz approach to examine the critical buckling load of the cylindrical shell formed of porous nanocomposite strengthened with graphene platelets. Zhang [25] examined the behavior of damping and free vibration for sandwich plates made of porous functionally graded materials corresponding to the modified Fourier-Ritz method. Heidari *et al.* [26] proposed an analytical method for studying the conduct of free vibration in small-scale circular cylindrical shells made of uniformly graded material and surrounded on both sides by a piezoelectric array. Akbaş *et al.* [27] investigated dynamic responses of a thick beam rested on the two viscoelastic supports formed of porous functionally graded layers under sine pulse load. Ebrahimi *et al*. [28] described an analytical solution to explain the characteristic behavior of free vibration for sandwich plates manufactured from three layers; the middle layer is made of functionally graded carbon nanotubes strengthened with composites, and the other two layers are made of porous magneto-electro-elastic (MEE) functionally graded. Cong and Duc [29] displayed an analytical approach to explain the amplitude of non-linear dynamic vibrations for double-curved shallow shells surrounded on one face by porous eccentrically stiffened placed on the Visco-Pasternak foundation under the influence of thermal environments. Njim *et al*. [30-31] presented an analytical and numerical study of the free vibration and buckling characterization of the sandwich plate with an FG porous metal core. According to the authors' knowledge and literature, it was found that a few works have been conducted previously to investigate the behavior of nonlinear vibration responses of porose FGM cylindrical panels, and most researchers considered that the structure is in the form of a sandwich and the porosity is either in the core or in the two outer layers. Therefore, the originality of this research is that the cylindrical panels consist of a single layer made of FGM that includes a regular distribution of porosity. In this study, an analytical method was developed to predict the characterization of the nonlinear dynamic's response for porous FGM cylindrical shells. Based on the classical shell theory, equations of motion are obtained. In the numerical approach, the Galerkin technique and the fourth-order Runge-Kutta are conducted to provide the expression of natural frequencies and amplitudes of nonlinear vibration response by writing a code in MATLAB software. Several factors that affect free and force nonlinear vibration are looked at, such as the porosity parameter, power-law index, porous FGM thickness, Frequency–amplitude relation, and the force that is used to move it. The numerical results are compared to the approximate solution to see if the method used is correct.

1.1 Porous Functionally Graded Cylindrical Panel

A schematic of the porous FG cylindrical panel utilized in the present analysis is displayed in Figure 1. The uniform thickness h, the length of the edges a and b, and the radius of curvature R of the cylindrical panel. There's also a coordinate system set up between the outside and inside of the panel: (x,y,z).

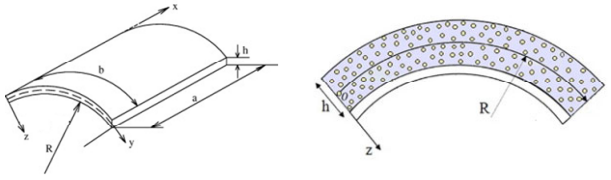

a) Cartesian coordinate system b) Porosity with even distribution

Figure 1 A schematic of the PFGM cylindrical panel

To achieve the condition of the functionally graded material, there are several laws, including power-law, exponential law, and sigmoid law variation. In this study, it is assumed that FGMs are a mixture of ceramic and metal according to the power-law distribution [32]:

$$V_m + V_c = 1, V_c = V_c(z) = \left(\frac{2z+h}{2h}\right)^k, \tag{1}$$

Where (V_c and V_m) refer to volume fractions of ceramic and metal, respectively. In addition, an important parameter (k) is called the volume fraction index, and the value of this parameter is [0, a), non-negative, where the value is equal to infinite, it means a fully metallic shell, whereas zero denotes a fully ceramic shell. The FGM cylindrical panel is supposed to carry porosities that are distributed unevenly or evenly along the thickness direction of the cylindrical shell. The properties of the materials of the FGM cylindrical panel with porosities are graded continuously toward the thickness direction of the shell corresponding to the power-law distribution. The material properties such as Young's modulus E (z), the mass density for the even or uniform distribution of porosities of the imperfect FGM shell can be defined, respectively, as [33]:

$$E(z) = E_m V_m + E_c V_c = E_m + (E_c - E_m)\left(\frac{2z+h}{2h}\right)^k - \frac{\beta}{2}(E_c - E_m),$$
$$\rho(z) = \rho_m V_m + \rho_c V_c = \rho_m + (\rho_c - \rho_m)\left(\frac{2z+h}{2h}\right)^k - \frac{\beta}{2}(\rho_c + \rho_m), \tag{2}$$

2.0 METHODOLOGY

In this study, the classical shell theory (CST) is employed to derive the governing equations of motion for the non-linear dynamic response of porous FGM cylindrical panels. The displacement field of the porous FGM cylindrical panels that are based on the CST can be sold as a service as [34]:

$$\hat{u}(x,y,z,t) = u(x,y,t) - z\left(\frac{\partial w}{\partial x}\right),$$
$$\hat{v}(x,y,z,t) = v(x,y,t) - z\left(\frac{\partial w}{\partial y}\right), \tag{3}$$
$$\hat{w}(x,y,z,t) = w(x,y,t),$$

Where (u,v,w) denote the displacement components concerning the coordinates (x,y,z) respectively; and t is the time. Employing the above displacements, the strain–displacement relations of the system, taking into account the von Karman nonlinearity, is shown as [35]:

$$\begin{pmatrix} \varepsilon_x \\ \varepsilon_y \\ \gamma_{xy} \end{pmatrix} = \begin{pmatrix} \varepsilon_x^\circ \\ \varepsilon_y^\circ \\ \gamma_{xy}^\circ \end{pmatrix} - z \begin{pmatrix} \lambda_x \\ \lambda_y \\ 2\lambda_{xy} \end{pmatrix}, \tag{4}$$

With

$$\begin{pmatrix} \varepsilon_x^\circ \\ \varepsilon_y^\circ \\ \gamma_{xy}^\circ \end{pmatrix} = \begin{pmatrix} \frac{\partial u}{\partial x} + \frac{1}{2}\left(\frac{\partial w}{\partial x}\right)^2 \\ \frac{\partial v}{\partial y} - \frac{w}{R} + \frac{1}{2}\left(\frac{\partial w}{\partial x}\right)^2 \\ \frac{\partial u}{\partial y} + \frac{\partial v}{\partial x} + \frac{\partial w}{\partial x}\frac{\partial w}{\partial y} \end{pmatrix}, \begin{pmatrix} \lambda_x \\ \lambda_y \\ \lambda_{xy} \end{pmatrix} = \begin{pmatrix} \frac{\partial^2 w}{\partial x^2} \\ \frac{\partial^2 w}{\partial y^2} \\ \frac{\partial^2 w}{\partial x\,\partial y} \end{pmatrix}, \tag{5}$$

$(\varepsilon_x, \varepsilon_y and\ \gamma_{xy})$ describe the normal strains and shear strain respectively of the cylindrical panels. According to equation (4), the strains must be comparable to the compatibility deformation equation.

$$\frac{\partial^2 \varepsilon_x^\circ}{\partial x^2} + \frac{\partial^2 \varepsilon_y^\circ}{\partial y^2} - \frac{\partial^2 \gamma_{xy}^\circ}{\partial x\,\partial y} = \left(\frac{\partial^2 w}{\partial x\,\partial y}\right)^2 - \frac{\partial^2 w}{\partial x^2}\frac{\partial^2 w}{\partial y^2} - \frac{1}{R}\frac{\partial^2 w}{\partial x^2}, \tag{6}$$

For a cylindrical shell, Hooke's law is defined by [36]:

$$\sigma_x = \frac{E(z)}{1-\nu^2}(\varepsilon_x + \nu\varepsilon_y),$$
$$\sigma_y = \frac{E(z)}{1-\nu^2}(\varepsilon_y + \nu\varepsilon_x), \tag{7}$$
$$\tau_{xy} = \frac{E(z)}{2(1+\nu)}\gamma_{xy},$$

Integrating the equations for stress-strain and their moments through the thickness directions of a cylindrical shell made of porous FGM can help figure out the force and moment resultants of the shell.

$$N_x = I_{10}\varepsilon_x^\circ + I_{20}\varepsilon_y^\circ - I_{11}\lambda_x - I_{21}\lambda_y, \tag{8a}$$
$$N_y = I_{20}\varepsilon_x^\circ + I_{10}\varepsilon_y^\circ - I_{21}\lambda_x - I_{11}\lambda_y, \tag{8b}$$
$$N_{xy} = I_{30}\gamma_{xy}^\circ - 2I_{31}\lambda_{xy}, \tag{8c}$$
$$M_x = I_{11}\varepsilon_x^\circ + I_{21}\varepsilon_y^\circ - I_{12}\lambda_x - I_{22}\lambda_y, \tag{9a}$$
$$M_y = I_{21}\varepsilon_x^\circ + I_{11}\varepsilon_y^\circ - I_{22}\lambda_x - I_{12}\lambda_y, \tag{9b}$$
$$M_{xy} = I_{31}\gamma_{xy}^\circ - 2I_{32}\lambda_{xy}, \tag{9c}$$

The coefficients in equations (8 & 9) are explained in Appendix. The relations of the strain-force resultant reversely are got from Equation (8):

$$\begin{aligned}\varepsilon_x^\circ &= A_{22}N_x - A_{12}N_y + B_{11}\lambda_x + B_{12}\lambda_y,\\ \varepsilon_y^\circ &= A_{11}N_y - A_{12}N_x + B_{21}\lambda_x + B_{22}\lambda_y,\\ \gamma_{xy}^\circ &= A_{66}N_{xy} + 2B_{66}\lambda_{xy},\end{aligned} \tag{10}$$

Substituting Equation (10) into Equation (9) we obtain:

$$\begin{aligned}M_x &= B_{11}N_x + B_{21}N_y - D_{11}\lambda_x - D_{12}\lambda_y,\\ M_y &= B_{12}N_x + B_{22}N_y - D_{21}\lambda_x - D_{22}\lambda_y,\\ M_{xy} &= B_{66}N_{xy} - 2D_{66}N_{xy},\end{aligned} \tag{11}$$

The coefficients (A_{ij}, B_{ij}, D_{ij}) are illustrated in Appendix.

The nonlinear equations of motion of the porous FGM cylindrical shell according to (CST) and the assumption u≪w, and v≪w [37], [38] led to:

$$\rho_1\frac{\partial^2 u}{\partial t^2}\to 0, \rho_1\frac{\partial^2 v}{\partial t^2}\to 0$$

$$\frac{\partial N_x}{\partial x}+\frac{\partial N_{xy}}{\partial y}=0, \tag{12a}$$

$$\frac{\partial N_{xy}}{\partial x}+\frac{\partial N_y}{\partial y}=0, \tag{12b}$$

$$\begin{aligned}&\frac{\partial^2 M_x}{\partial x^2}+2\frac{\partial^2 M_{xy}}{\partial x\partial y}+\frac{\partial^2 M_y}{\partial y^2}+N_x\frac{\partial^2 w}{\partial x^2}+2N_{xy}\frac{\partial^2 w}{\partial x\partial y}+\\ &N_y\frac{\partial^2 w}{\partial y^2}+q+\frac{N_y}{R}=\rho_1\frac{\partial^2 w}{\partial t^2},\end{aligned} \tag{12c}$$

The first two equations are solved directly after employing the stress function as follows [15]:

$$N_x=\frac{\partial^2\varphi}{\partial y^2}, N_y=\frac{\partial^2\varphi}{\partial x^2}, N_{xy}=-\frac{\partial^2\varphi}{\partial x\partial y}, \tag{13}$$

Now substituting equation (10) into the compatibility equation (6), and equation (11) into the third part of the equation (12), taking into account the terms of equation (5), we obtain:

$$\begin{aligned}&A_{11}\frac{\partial^4 f}{\partial x^4}+(A_{66}-2A_{12})\frac{\partial^4 f}{\partial x^2\partial y^2}+A_{22}\frac{\partial^4 f}{\partial y^4}+B_{21}\frac{\partial^4 w}{\partial x^4}\\ &+(B_{11}+B_{22}-2B_{66})\frac{\partial^4 w}{\partial x^2\partial y^2}+B_{12}\frac{\partial^4 w}{\partial y^4}+\frac{1}{R}\frac{\partial^2 w}{\partial x^2}\\ &=\left(\frac{\partial^2 w}{\partial x\partial y}\right)^2-\frac{\partial^2 w}{\partial x^2}\frac{\partial^2 w}{\partial y^2},\end{aligned} \tag{14}$$

$$\begin{aligned}&\rho_1\frac{\partial^2 w}{\partial t^2}+D_{11}\frac{\partial^4 w}{\partial x^4}+(D_{12}+D_{21}+4D_{66})\frac{\partial^4 w}{\partial x^2\partial y^2}+D_{22}\frac{\partial^4 w}{\partial y^4}\\ &-B_{21}\frac{\partial^4 f}{\partial x^4}-(B_{11}+B_{22}-2B_{66})\frac{\partial^4 f}{\partial x^2\partial y^2}-B_{12}\frac{\partial^4 f}{\partial y^4}-\frac{1}{R}\frac{\partial^2 f}{\partial x^2}\\ &-\frac{\partial^2 f}{\partial y^2}\frac{\partial^2 w}{\partial x^2}+2\frac{\partial^2 f}{\partial x\partial y}\frac{\partial^2 w}{\partial x\partial y}-\frac{\partial^2 f}{\partial x^2}\frac{\partial^2 w}{\partial y^2}=q,\end{aligned} \tag{15}$$

Hereafter, the above two equations (14 and 15) are applied to analyze the behavior of the nonlinear vibration response of the porous cylindrical panels. It indicates that they are nonlinear equations with two dependent unknowns.

2.1 Decoupling Procedure

In this paper, the simply supported boundary conditions (SSSS) for the porous FG cylindrical panel subjected to uniformly distributed pressure (q°) are applied [17]:

$$\begin{aligned}&w=0, M_x=0, N_x=0, N_{xy}=0, at\ x=0, a,\\ &w=0, M_y=0, N_y=0, N_{xy}=0, at\ y=0, b,\end{aligned} \tag{16}$$

The above conditions can be fulfilled identically if the mode shape is expressed by [17]:

$$w=W(t)\sin\left(\frac{m\pi x}{a}\right)\sin\left(\frac{n\pi y}{b}\right), \tag{17}$$

Where, m, n=1, 2... represents the natural number of half-waves in the axial and circumferential directions, respectively. By substituting equation (17) in equation (14), and solving the equation for the unknown (f), we get:

$$\begin{aligned}&f(x,y,t)=\Psi_1\cos(2\lambda_m x)+\Psi_2\cos(2\delta_n y)+\\ &\Psi_3\sin(\lambda_m x)\sin(\delta_n y),\end{aligned} \tag{18}$$

Where $\lambda_m=\frac{m\pi}{a}, \delta_n=\frac{n\pi}{b},$ and (ψ1, ψ2, ψ3) are defined in Appendix.

Equations (17 and 18) are substituted into equation (15), a complex differential equation will be produced. In order to simplify the resulting equation, we use the Calerkin method. This method converts a continuous operator problem, such as a differential equation, commonly into a weak formulation as:

$$\int_0^b\int_0^a[complex\ equation]\sin\left(\frac{m\pi x}{a}\right)\sin\left(\frac{n\pi y}{b}\right)dxdy, \tag{19}$$

Next, we solve this equation by utilizing Galerkin's procedure as follows:

$$\begin{aligned}&M\ddot{W}+\left(D+\frac{B^2}{A}\right)W+\frac{8mn\lambda^2}{3\pi^2}\frac{B}{A}\delta_1\delta_2W^2+HW^2+\\ &KW^3-\frac{4qa^4}{mn\pi^6}\delta_1\delta_2=0,\end{aligned} \tag{20}$$

All coefficients in equation (20) are displayed in the Appendix. The above equation is used to study and analyze the non-linear behavior of cylindrical panels made of porous FGM. It is the main equation for this.

2.2 Vibration Analysis

Taking into account that porous FGM cylindrical panels are exposed to uniformly distributed load (q= Q sin Ωt), the non-linear Equation (19) becomes:

$$M\ddot{W}+\left(D+\frac{B^2}{A}\right)W+\frac{8mn\lambda^2}{3\pi^2}\frac{B}{A}\delta_1\delta_2W^2+HW^2 \quad (21)$$
$$+KW^3=\frac{4qa^4}{mn\pi^6}\delta_1\delta_2,$$

Using Equation (21), three important and main parameters are taken into account: natural frequencies, nonlinear free vibration, and the frequency–amplitude) relation of the nonlinear response of a porous FGM shell. The responses of porous FGM shells can be determined by solving the above equation with the initial conditions W (0) =0 by adopting the Runge–Kutta technique. For free vibration, Equation (20) is rewritten as:

$$M\ddot{W}+\left(D+\frac{B^2}{A}\right)W=0, \quad (21)$$

The linear fundamental natural frequencies of porose FGM cylindrical panels can be calculated as:

$$\omega_L=\sqrt{\frac{1}{M}\left(D+\frac{B^2}{A}\right)}, \quad (22)$$

The equation of non-linear for free vibration can be obtained as follow:

$$\ddot{W}+S_1W+S_2W^2+S_3W^3=0, \quad (23)$$

Where:

$$S_1=\omega_L{}^2=\frac{1}{M}\left(D+\frac{B^2}{A}\right), \quad (24)$$
$$S_2=\frac{1}{M}\left(\frac{3mn\lambda^2}{3\pi^2}\frac{B}{A}\delta_1\delta_2+H\right),S_3=\frac{K}{M},$$

The Galerkin's method is used to figure out how the frequencies and amplitudes of nonlinear free vibration are related. We do this by putting equation (23) in the same way of equation (20): W(t)=η cos (ωt).

$$\omega_{NL}=\omega_L\left(1+\frac{8S_2}{3\pi\omega_L{}^2}\eta+\frac{3S_3}{4\omega_L{}^2}\eta^2\right)^{\frac{1}{2}}, \quad (25)$$

Where (ωNL) Expresses the nonlinear frequencies of free vibration, and (η) describes the amplitude of nonlinear vibration.

3.0 RESULTS AND DISCUSSION

3.1 Comparison Studies

Since no current study has been conducted on characterizations of the nonlinear vibration of the FG layer made of the porous ceramic-metal cylindrical shell, the comparison of the dimensionless natural frequency offered by the current analysis with the result of Matsunaga [39] based on the (2D) higher-order theory, Chorfi and Haumat [40] based on the (FSDT), Alijani *et al*. [41]based on Donnell's non-linear doubly curved shallow shell theory, and Duc [42] based on classical shell theory for the perfect unreinforced (FGM) cylindrical shells are conducted for validation of the present technique. The results in Table 1 were gained with [a/b=1, h/a=0.1 ,Ec=380×10^9 N/m^2 ,Em=70×10^9 N/m^2 ,ρc= 3800 kg/m^3 ,ρm=2702 kg/m^3]. A very good agreement in this comparative investigation can be seen in Table 1.

Table 1 Comparison of the dimensionless natural frequency with results reported by Matsunaga [39], Chorfi and Houmat [40], Alijani *et al*. [41], and Duc [42]

a/R	k	Ref [39]	Ref [40]	Ref [41]	Ref [42]	Present
FGM plat 0	0	0.0588	0.0577	0.0597	0.0562	0.0597
	0.5	0.0492	0.0490	0.0506	0.0502	0.0506
	1	0.0403	0.0442	0.0456	0.0449	0.0456
	4	0.0381	0.0383	0.0396	0.0385	0.0396
	10	0.0364	0.0366	0.0380	0.0304	0.0381
FGM cylindrical panel 0.5	0	0.0622	0.0629	0.0648	0.0624	0.0648
	0.5	0.0535	0.0540	0.0553	0.0528	0.0553
	1	0.0485	0.0490	0.0501	0.0494	0.0501
	4	0.0413	0.0419	0.0430	0.0407	0.0430
	10	0.0390	0.0395	0.0408	0.0379	0.0409

3.2 Free Vibration and Dynamic Response of Cylindrical Porous FG Cylindrical Panels

In this part, some numerical models are presented to examine the nonlinear dynamic response and characteristics of the natural frequency of porous FG cylindrical panels. The porous FG layer considered here consists of aluminum and alumina, and the material properties are detailed in Table 2.

Table 2 Material properties utilized in the porous FG cylindrical panels

Property	Aluminum (Al)	Ceramic (Al2O3)
Modula's of Elasticity, GPa	70	380
Mass density, Kg/m3	2702	3800
Poisson's ratio	0.3	0.3

Table 3 displays the effect of increasing the porosity and the power index on the natural frequencies of functionally graded cylindrical panels.

The porosity parameters (0, 0.1, 0.2, 0.3, and 0.4) and power-law indices (0, 0.5, 1, 2, 10). The FGM thickness h=0.008 m. It is evident from this table that increasing the porosity parameter yields decreasing in the natural frequency due to the reduction in the bending rigidity of the FG shell. In addition, the natural frequencies decrease with the increase of the power-law index and the reason for this is that when the value of the power-law index increases, the young modulus of the Aluminum will increase in this layer according to the equation (2, and as it is known that the modulus of elasticity of Aluminum is less than Alumina. As is anticipated, with an increase in the (k), the cylindrical shell's elasticity modulus and bending rigidity decrease. So, the material strength decreases.

Figure 2 illustrates the influence of increasing the porosity on the displacement-time response. First, four values of porosity are analyzed (without porosity, 10%, 20%, and 30%). This figure demonstrates that increasing the porosity leads to an increase in the amplitude of nonlinear vibration. In other words, the deflection will increase due to the decreased strength of the material as a result of increasing the voids. where the increase in the height of the curve reaches 32%.

Table 3 Analytical results of the natural frequencies of (Al/ Al2O3) cylindrical panels for various parameters. a=b=1.5 m, R=3 m, h=0.008 m

Porosity	Power-law index				
%	0	0.5	1	2	10
0	1680.1	1506.8	1396	1261.4	995.8527
0.1	1672	1481	1358	1206.6	896.9094
0.2	1662.9	1452.9	1315.2	1142.4	771.7536
0.3	1652.6	1420.3	1265.2	1065.9	599.6844

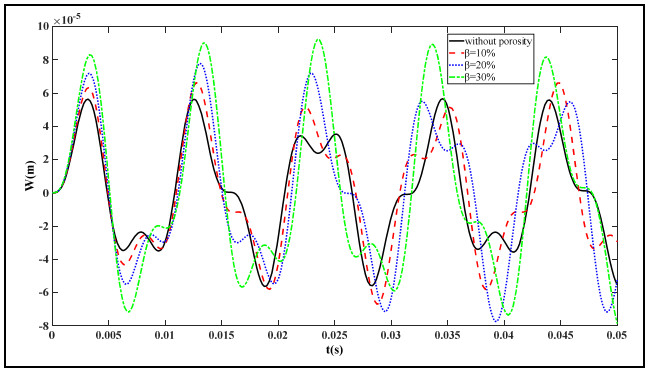

Figure 2 Effect of porosity parameter on the nonlinear time-displacement response for FGM cylindrical panel. R=3 m, h= 0.01 m, a=b=1.5 m

Another result can be found in Figure 3, which displays the influence of the increase in power index and porosity parameter on the time-displacement curve. The power index (0.5, 1, and 2), where the gradient condition is satisfied and at the same time the porosity values (0%, 10%, and 20%). The material distribution parameter (k) is significantly influential on the nonlinear dynamics response. An increasing volume fraction index leads to an increase in the amplitude of nonlinear vibration, meaning that the displacement will increase due to the increase in the percentage of metal in the layer of the shell.

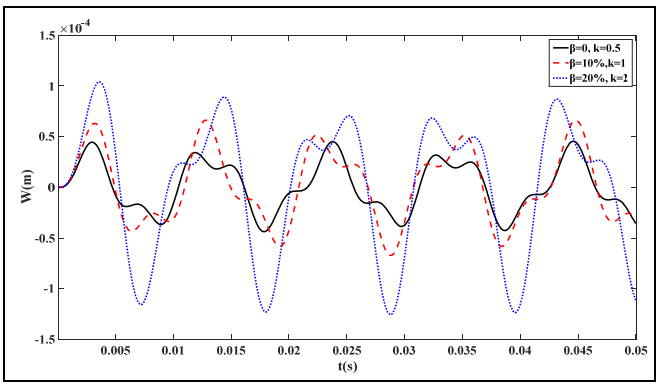

Figure 3 Influence of power index and porosity parameter on the nonlinear time-displacement response for FGM cylindrical panel. R=3 m, h= 0.01 m, a=b=1.5 m

Figure 4 represents the effect of an increase in the thickness of the porous FGM layer on the nonlinear dynamic behavior of cylindrical shells. With a percentage of porosity of 20% and a value of material distribution parameter of 0.5 to achieve the condition of gradation between the two materials, it was found that increasing the thickness of the porous FGM layer from 0.01 m to 0.03 m leads to a decrease in the amplitude of vibrations. Therefore, the shell becomes more rigid and this indicates that the value of the natural frequencies will be increased.

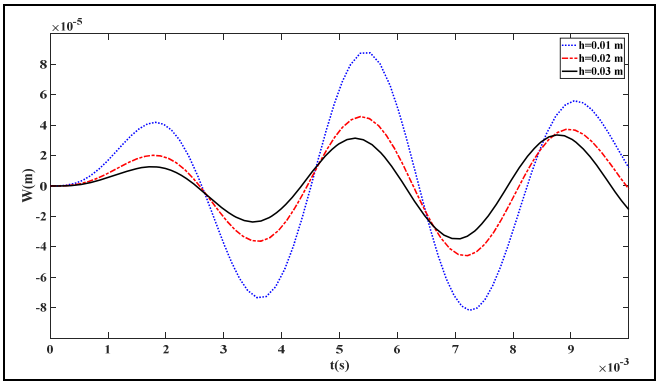

Figure 4 Effect of porous FGM layer on the nonlinear time-displacement response of shell. R=3 m, a=b=1.5 m, β=20 %, k=0.5

Figure 5 displays the relationship between the frequency and amplitude of nonlinear free vibration with the porosity effect of a cylindrical panel was evaluated according to equation (25) with k = 0.5, m = 1, and n=1. As expected, the nonlinear free vibration frequencies of panels without porosity

(perfect) panels are greater than those of panels with porosity.

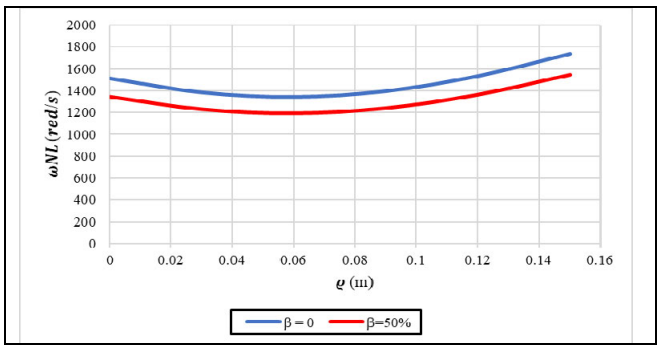

Figure 5 Frequency–amplitude relation

The influence of the harmonic uniform load (Q) on the time-displacement response of porose FGM cylindrical panels is represented in Figure 6. Three values of (Q) are employed as (Q=1000 N/m2, Q=2000 N/m2, Q=3000 N/m2). Under the influence of increased excitation force, the three types of reinforcement are thought to behave in the same way. It can be seen that the excitation force has a strong impact on the vibration response. When raising the excitation force, the vibration amplitude will increase greatly.

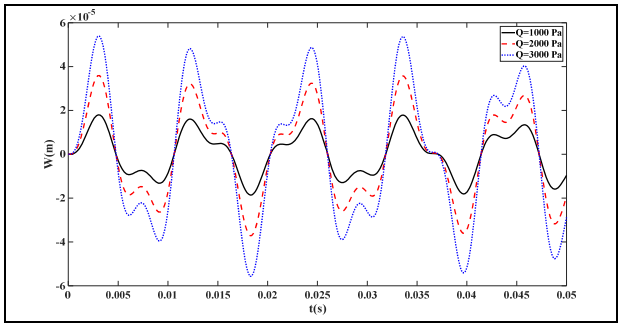

Figure 6 Effect of excitation force (Q) on the nonlinear time-displacement response for porous FGM cylindrical panel. a=b=1.5 m, k=0.5, R=3 m, h=0.01 m, Ω=600

4.0 CONCLUSION

In the current work, fundamental natural frequencies and non-linear dynamic responses of functionally graded porous ceramic-metal shells are theoretically analyzed employing the classical thin shell theory. The numerical Galerkin method and fourth-order Runge–Kutta technique is exploited to solve the governing equation of motion incrementally by writing a code in the MATLAB program. The properties of the material are graded continuously with porosity through the shell thickness and modeled by the power-law distributions. Based on the results, the following observations are made: (1) It can be observed that the natural frequencies of the shell decrease by 5.74% with the increased porous characteristics by 10 % because of a reduction in bending rigidity (2) An increase in material distribution parameters led to a decrease in the natural frequencies due to a rise in the volumetric percentage of the metal (3) Increasing both the porosity and volume fraction index leads to an increase in the amplitude of nonlinear vibration response (4) The layer thickness of porous FGMs has a significant effect on the time-displacement curve, as increasing the thickness leads to a decrease in the response curve (5) The non-linear vibration frequencies of shells without porosity are greater than those of shells with porosity (6) When the structure is hit with an excitation force, the time-displacement curve will change a lot.

References

[1] S. Hosseini-Hashemi, A. R. Abaei, and M. R. Ilkhani. 2015. Free Vibrations of Functionally Graded Viscoelastic Cylindrical Panel under Various Boundary Conditions. *Composite Structures*. 126: 1-15. Doi: 10.1016/j.compstruct.2015.02.031.

[2] I. M. El-Galy, B. I. Saleh, and M. H. Ahmed. 2019. Functionally Graded Materials Classifications and Development Trends from Industrial Point of View. *SN Applied Sciences*. 1(11). Springer Nature. Doi: 10.1007/s42452-019-1413-4.

[3] K. Gao, Q. Huang, S. Kitipornchai, and J. Yang. 2021. Nonlinear Dynamic Buckling of Functionally Graded Porous Beams. *Mechanics of Advanced Materials and Structures*. 28(4): 418-429. Doi: 10.1080/15376494.2019.1567888.

[4] Soldatos, K. P., and V. P. Hadjigeorgiou. 1990. Three-dimensional Solution of the Free Vibration Problem of Homogeneous Isotropic Cylindrical Shells and Panels. *Journal of Sound and Vibration*. 137(3): 369-384.

[5] J. A. Zukas and J. R. Vinson. 1971. Laminated Transversely Isotropic Cylindrical Shells. [Online]. Available: http://www.asme.org/about-asme/terms-of-use.

[6] Bich, Dao Huy. 2006. Non-linear Analysis of Laminated Composite Doubly Curved Shallow Shells. *Vietnam Journal of Mechanics*. 28(1): 43-55.

[7] S. M. R. Khalili, A. Davar, and K. Malekzadeh Fard. 2012. Free Vibration Analysis of Homogeneous Isotropic Circular Cylindrical Shells Based on a New Three-Dimensional Refined Higher-Order Theory. *International Journal of Mechanical Sciences*. 56(1): 1-25. Doi: 10.1016/j.ijmecsci.2011.11.002.

[8] A. G. Shah, T. Mahmood, and M. N. Naeem. 2009. Vibrations of FGM Thin Cylindrical Shells with Exponential Volume Fraction Law. *Applied Mathematics and Mechanics (English Edition)*. 30(5): 607-615. Doi: 10.1007/s10483-009-0507-x.

[9] S. H. Arshad, M. N. Naeem, N. Sultana, A. G. Shah, and Z. Iqbal. 2011. Vibration Analysis of bi-layered FGM Cylindrical Shells. *Archive of Applied Mechanics*. 81(3): 319-343. Doi: 10.1007/s00419-010-0409-8.

[10] A. H. Sofiyev. 2011. On the Vibration and Stability of Clamped FGM Conical Shells Under External Loads. *Journal of Composite Materials*. 45(7): 771-788. Doi: 10.1177/0021998310373515.

[11] H. S. Shen. 2012. Nonlinear Vibration of Shear Deformable FGM Cylindrical Shells Surrounded by an Elastic Medium. *Composite Structures*. 94(3): 1144-1154. Doi: 10.1016/j.compstruct.2011.11.012.

[12] Loy, C. T., K. Y. Lam, and J. N. Reddy. 1999. Vibration of Functionally Graded Cylindrical Shells. *International Journal of Mechanical Sciences.* 41(3): 309-324.
[13] Bich, Dao Huy. 2006. Non-linear Analysis of Laminated Composite Doubly Curved Shallow Shells. *Vietnam Journal of Mechanics.* 28(1): 43-55.
[14] S. M. Chorfi and A. Houmat. 2010. Non-linear Free Vibration of a Functionally Graded Doubly-curved Shallow Shell of Elliptical Plan-form. *Composite Structures*. 92(10): 2573-2581. Doi: 10.1016/j.compstruct.2010.02.001.
[15] Mouthanna, Ahmed, Hamad M. Hasan, and Khalid B. Najim. 2018. Nonlinear Vibration Analysis of Functionally Graded Imperfection of Cylindrical Panels Reinforced with Different Types of Stiffeners. *2018 11th International Conference on Developments in eSystems Engineering (DeSE). IEEE.*
[16] S. R. Li, X. H. Fu, and R. C. Batra. 2010. Free Vibration of Three-layer Circular Cylindrical Shells with Functionally Graded Middle Layer. *Mechanics Research Communications*. 37(6): 577-580. Doi: 10.1016/j.mechrescom.2010.07.006.
[17] D. H. Bich, D. van Dung, and V. H. Nam, Jul. 2012 Nonlinear Dynamical Analysis of Eccentrically Stiffened Functionally Graded Cylindrical Panels. *Composite Structures*. 94(8): 2465-2473. Doi: 10.1016/j.compstruct.2012.03.012.
[18] N. D. Duc and T. Q. Quan. 2014. Nonlinear Response of Imperfect Eccentrically Stiffened FGM Cylindrical Panels on Elastic Foundation Subjected to Mechanical Loads. *European Journal of Mechanics, A/Solids*. 46: 60-71. Doi: 10.1016/j.euromechsol.2014.02.005.
[19] D. Wu, A. Liu, Y. Huang, Y. Huang, Y. Pi, and W. Gao, Jun. 2018. Dynamic Analysis of Functionally Graded Porous Structures through Finite Element Analysis. *Engineering Structures*. 165: 287-301. Doi: 10.1016/j.engstruct.2018.03.023.
[20] Ş. D. Akbaş, Feb. 2018. Forced Vibration Analysis of Functionally Graded Porous Deep Beams. *Composite Structures*. 186: 293-302. Doi: 10.1016/j.compstruct.2017.12.013.
[21] H. Li, F. Pang, H. Chen, and Y. Du. 2019. Vibration Analysis of Functionally Graded Porous Cylindrical Shell with Arbitrary Boundary Restraints by using a Semi Analytical Method. *Composites Part B: Engineering*. 164: 249-264. Doi: 10.1016/j.compositesb.2018.11.046.
[22] M. R. Barati and A. M. Zenkour. 2019. Vibration Analysis of Functionally Graded Graphene Platelet Reinforced Cylindrical Shells with Different Porosity Distributions. *Mechanics of Advanced Materials and Structures*. 26(18): 1580-1588. Doi: 10.1080/15376494.2018.1444235.
[23] D. Akbaş, Y. A. Fageehi, A. E. Assie, and M. A. Eltaher. 2020. Dynamic Analysis of Viscoelastic Functionally Graded Porous Thick Beams Under Pulse Load. *Engineering with Computers*. Doi: 10.1007/s00366-020-01070-3.
[24] D. Shahgholian, M. Safarpour, A. R. Rahimi, and A. Alibeigloo. 2020. Buckling Analyses of Functionally Graded Graphene-reinforced Porous Cylindrical Shell using the Rayleigh–Ritz Method. *Acta Mechanica*. 231(5): 1887-1902. Doi: 10.1007/s00707-020-02616-8.
[25] Y. Zhang, G. Jin, M. Chen, T. Ye, C. Yang, and Y. Yin, Jul. 2020. Free Vibration and Damping Analysis of Porous Functionally Graded Sandwich Plates with a Viscoelastic Core. *Composite Structures*. 244. Doi: 10.1016/j.compstruct.2020.112298.
[26] Y. Heidari, M. Arefi, and M. Irani Rahaghi. 2020. Nonlocal Vibration Characteristics of a Functionally Graded Porous Cylindrical Nanoshell Integrated with Arbitrary Arrays of Piezoelectric Elements. *Mechanics Based Design of Structures and Machines*. Doi: 10.1080/15397734.2020.1830799.
[27] Ş. D. Akbaş, A. H. Bashiri, A. E. Assie, and M. A. Eltaher. 2021. Dynamic Analysis of Thick Beams with Functionally Graded Porous Layers and Viscoelastic Support. *JVC/Journal of Vibration and Control*. 27(13-14): 1644-1655. Doi: 10.1177/1077546320947302.
[28] F. Ebrahimi, N. Farazmandnia, M. R. Kokaba, and V. Mahesh. 2021. Vibration Analysis of Porous Magneto-electro-elastically Actuated Carbon Nanotube-reinforced Composite Sandwich Plate based on a Refined Plate Theory. *Engineering with Computers*. 37(2): 921-936. Doi: 10.1007/s00366-019-00864-4.
[29] P. H. Cong and N. D. Duc. 2021. Nonlinear Dynamic Analysis of Porous Eccentrically Stiffened Double Curved Shallow Auxetic Shells in Thermal Environments. *Thin-Walled Structures*. 163. Doi: 10.1016/j.tws.2021.107748.
[30] Njim, E. K., Bakhy, S. H., & Al-Waily, M. 2021. Analytical and Numerical Investigation of Free Vibration Behavior for Sandwich Plate with Functionally Graded Porous Metal Core. *Pertanika Journal of Science & Technology*. 29(3).
[31] Njim, E. K., Bakhy, S. H., & Al-Waily, M. 2021. Analytical and Numerical Investigation of Buckling Behavior of Functionally Graded Sandwich Plate with Porous Core. *Journal of Applied Science and Engineering*. 25(2): 339-347.
[32] P. van Vinh. 2022. Nonlocal Free Vibration Characteristics of Power-law and Sigmoid Functionally Graded Nanoplates Considering Variable Nonlocal Parameter. *Physica E: Low-Dimensional Systems and Nanostructures*. 135. Doi: 10.1016/j.physe.2021.114951.
[33] Y. Zhang, G. Jin, M. Chen, T. Ye, C. Yang, and Y. Yin. 2020. Free Vibration and Damping Analysis of Porous Functionally Graded Sandwich Plates with a Viscoelastic Core. *Composite Structures*. 244. Doi: 10.1016/j.compstruct.2020.112298.
[34] D. H. Bich and D. G. Ninh. 2017. An Analytical Approach: Nonlinear Vibration of Imperfect Stiffened FGM Sandwich Toroidal Shell Segments Containing Fluid under External Thermo-mechanical Loads. *Composite Structures*. 162: 164-181. Doi: 10.1016/j.compstruct.2016.11.065.
[35] D. H. Bich, D. van Dung, and V. H. Nam. 2012. Nonlinear Dynamical Analysis of Eccentrically Stiffened Functionally graded Cylindrical Panels. *Composite Structures.* 94(8): 2465-2473. Doi: 10.1016/j.compstruct.2012.03.012.
[36] P. T. Thang and T. Nguyen-Thoi. 2016. A New Approach for Nonlinear Dynamic Buckling of S-FGM Toroidal Shell Segments with Axial and Circumferential Stiffeners. *Aerospace Science and Technology*. 53: 1-9. Doi: 10.1016/j.ast.2016.03.008.
[37] M. Darabi, M. Darvizeh, and A. Darvizeh. 2008. Non-linear Analysis of Dynamic Stability for Functionally Graded Cylindrical Shells under Periodic Axial Loading. *Composite Structures*. 83(2): 201-211. Doi: 10.1016/j.compstruct.2007.04.014.
[38] A. H. Sofiyev and E. Schnack. 2004. The Stability of Functionally Graded Cylindrical Shells under Linearly Increasing Dynamic Torsional Loading. *Engineering Structures*. 26(10): 1321-1331. Doi: 10.1016/j.engstruct.2004.03.016.
[39] H. Matsunaga. 2008. Free Vibration and Stability of Functionally Graded Shallow Shells according to a 2D Higher-order Deformation Theory. *Composite Structures*. 84(2): 132-146. Doi: 10.1016/j.compstruct.2007.07.006.
[40] S. M. Chorfi and A. Houmat. 2010. Non-linear Free Vibration of a Functionally Graded Doubly-curved Shallow Shell of Elliptical Plan-form. *Composite Structures*. 92(10): 2573-2581. Doi: 10.1016/j.compstruct.2010.02.001.
[41] F. Alijani, M. Amabili, K. Karagiozis, and F. Bakhtiari-Nejad. 2011. Nonlinear Vibrations of Functionally Graded Doubly Curved Shallow Shells. *Journal of Sound and Vibration*. 330(7): 1432-1454. Doi: 10.1016/j.jsv.2010.10.003.
[42] N. D. Duc. 2013. Nonlinear Dynamic Response of Imperfect Eccentrically Stiffened FGM Double Curved Shallow Shells on Elastic Foundation. *Composite Structures*, 99: 88-9. Doi: 10.1016/j.compstruct.2012.11.017.

Appendix

$$I_{10}=\frac{E_1}{1-\upsilon^2},I_{20}=\frac{\upsilon E_1}{1-\upsilon^2},I_{30}=\frac{E_1}{2(1+\upsilon)},I_{11}=\frac{E_2}{1-\upsilon^2},$$

$$I_{21}=\frac{\upsilon E_2}{1-\upsilon^2},I_{31}=\frac{E_2}{2(1+\upsilon)},I_{12}=\frac{E_3}{1-\upsilon^2},I_{22}=\frac{\upsilon E_3}{1-\upsilon^2},$$

$$I_{32}=\frac{E_3}{2(1+\upsilon)},E_1=\left(E_m+\frac{(E_c-E_m)}{k+1}\right)h-\frac{\beta h}{2}(E_c+E_m),$$

$$E_2=\frac{(E_c-E_m)kh^2}{2(k+1)(k+2)},$$

$$E_3=[\frac{E_m}{12}+(E_c-E_m)\left(\frac{1}{(k+3)}-\frac{1}{(k+2)}+\frac{1}{(4k+4)}\right)-\frac{\beta}{24}(E_c+E_m)]\mathrm{h}^3,$$

$$\rho_1=\int_{-h/2}^{h/2}\rho(z)dz=\rho_m h+\frac{(\rho_c-\rho_m)h}{(1+k)}-\frac{\beta h}{2}(\rho_c+\rho_m),$$

$$A_{11}=\frac{I_{10}}{\Delta},A_{22}=\frac{I_{10}}{\Delta},A_{12}=\frac{I_{20}}{\Delta},A_{66}=\frac{1}{I_{30}},\Delta=(I_{10})(I_{10})-I_{20}^2,$$

$$B_{11}=A_{22}I_{11}-A_{12}I_{21},B_{22}=A_{11}I_{11}-A_{12}I_{21},$$

$$B_{12}=A_{22}I_{21}-A_{12}I_{11},B_{21}=A_{11}I_{21}-A_{12}I_{11},B_{66}=\frac{I_{31}}{I_{30}},$$

$$D_{11}=I_{12}-B_{11}B_{12}-I_{21}B_{21},D_{22}=I_{22}-B_{22}I_{11}-I_{21}B_{12},$$

$$D_{12}=I_{22}-B_{12}I_{11}-I_{21}B_{22},D_{21}=I_{22}-B_{21}I_{11}-I_{21}B_{11},$$

$$D_{66}=I_{32}-I_{31}B_{66},M=\frac{a^4}{\pi^4}\rho_1,$$

$$A=A_{11}m^4+(A_{66}-2A_{12})m^2n^2\lambda^2+A_{22}n^4\lambda^4,$$

$$B=B_{21}m^4+(B_{11}+B_{22}-2B_{66})m^2n^2\lambda^2+B_{12}n^4\lambda^4-\frac{a^2}{\pi^2}\frac{1}{R}m^2,$$

$$D=D_{11}m^4+(D_{12}+D_{21}+4D_{66})m^2n^2\lambda^2+D_{22}n^4\lambda^4,$$

$$H=\left[\frac{2mn\lambda^2}{3\pi^2}\left(\frac{B_{21}}{A_{11}}+\frac{B_{12}}{A_{22}}\right)-\frac{a^2}{6\pi^4mn}\frac{n^2\lambda^2}{A_{11}}\frac{1}{R}\right]\delta_1\delta_2,$$

$$K=\frac{1}{16}\left(\frac{m^4}{A_{22}}+\frac{n^4\lambda^4}{A_{11}}\right),\lambda=\frac{a}{b},\delta_1=(-1)^m-1,\delta_2=(-1)^n-1,$$

$$\Psi_1=\frac{n^2\lambda^2}{32A_{11}m^2}W^2,\Psi_2=\frac{m^2}{32A_{22}n^2\lambda^2}W^2,$$

$$\Psi_3=\frac{(B_{21}m^4+(B_{11}+B_{22}-2B_{66})m^2n^2\lambda^2+B_{12}n^4\lambda^4-\frac{a^2}{\pi^2}\frac{1}{R}m^2)}{(\Gamma_{11}m^4+(A_{66}-2A_{12})m^2n^2\lambda^2+A_{22}n^4\lambda^4)}W,$$

ENGLISH SYMBOLS

Notation	Description	Units
a	Panel length	m
b	Span length	m
R	Panel radius	m
h	Panel thickness	m
c	Ceramic	
m	Metal	
Vc	Volume fraction of ceramic	
Vm	Volume fraction of metal	
k	Power law index	Unitless
x, y, z	Panel coordinates	m
E	Young modulus	N/ m2
E_m	Elastic modulus for metal	N/ m2
E_c	Elastic modulus for ceramic	N/ m2
u, v	Displacement components along x, y directions	m
w	The deflection of the panel	m
N_x, N_y N_{xy}	Forces resultants	Newton
M_x, M_y M_{xy}	Moment's resultants	N.m
I_{ij}	Coefficients explained in the Appendix	N/ m2
q	Uniformly distributed pressure of intensity	Pascal
φ	The stress function	
$\Gamma_{ij}, \Lambda_{ij}, \Xi_{ij}$	Coefficients described in the Appendix	N/ m2
m	Axial wave number	Unitless
n	Circumferential wave number	Unitless
$\xi, \mu,$	Coefficients described in the Appendix	
Q	Excitation force	N/ m2

GREEK SYMBOLS

Notation	Description	Units
ρ	Mass density	Kg/ m3
ν	Poisson's ratio	Unitless
$\varepsilon_x, \varepsilon_y$	The normal strains component	Unitless
γ_{xy}	The shear strain component	Unitless
σ	Stress component	N/ m2
τ	Shear stress component	N/ m2
Ω	Rotational velocity	Rad/s
ω_L	Linear fundamental frequencies	Hertz (HZ)
η	Amplitude of nonlinear vibration	m
ω_{NL}	Nonlinear vibration frequency	Hertz (HZ)
γ_{xz}, γ_{yz}	The transverse shear strains components in the planes(xz, yz)	
β	The factor of the Porosity	Unitless